

Microscopic Giant Dipole Response and Nuclear Level Densities within Covariant Energy Density Functional Theory

Yuan Tian*, Ruirui Xu, Xi Tao, Jimin Wang, Zhigang Ge

China Nuclear Data Center(CNDC)

China Institute of Atomic Energy(CIAE)

P.O.Box 275-41, Beijing 102413, P.R.China

E-Mail: tiany@ciae.ac.cn





Introduction

Giant dipole resonance

Nuclear Level Densities

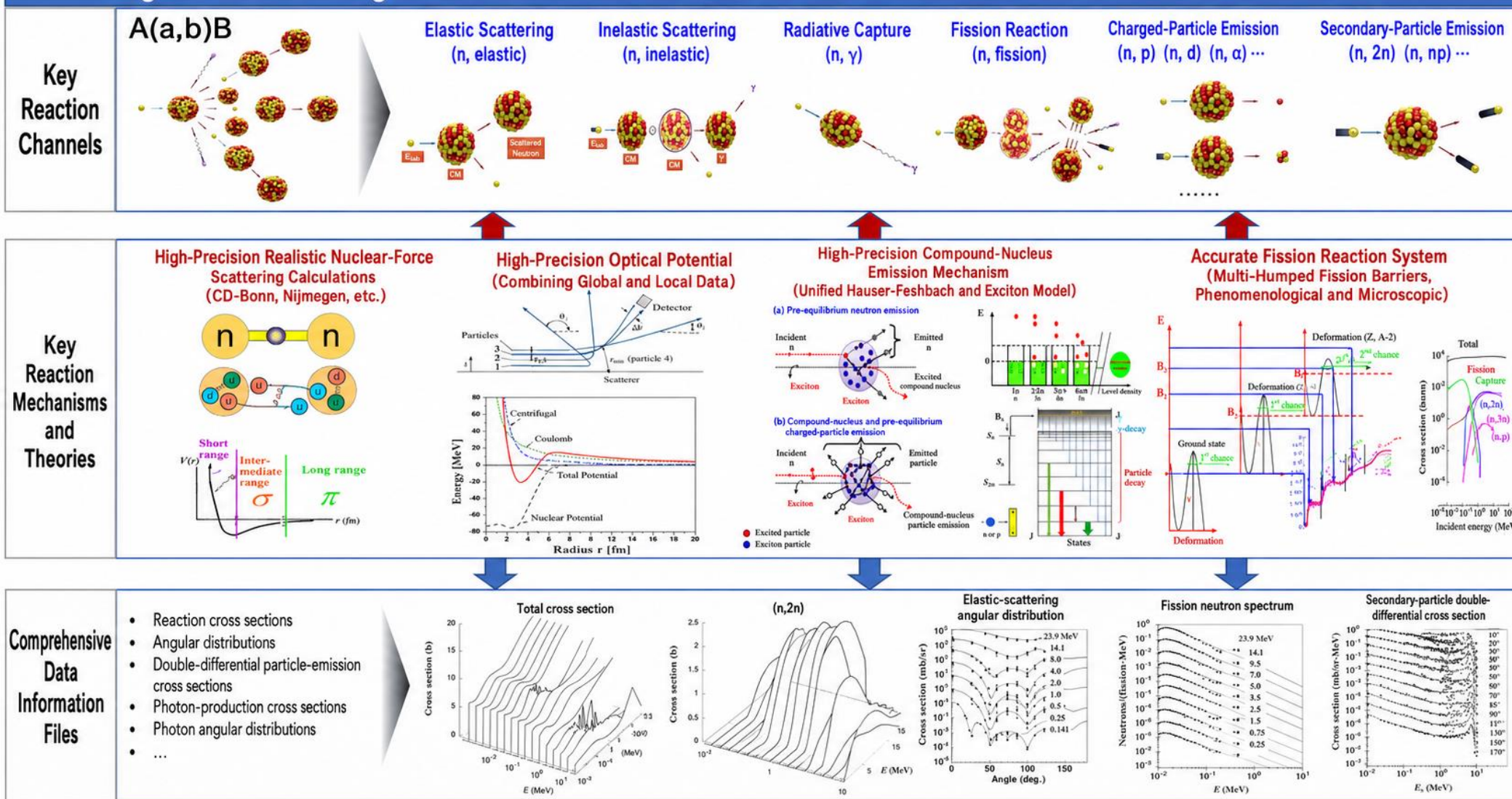
Conclusion and outlook



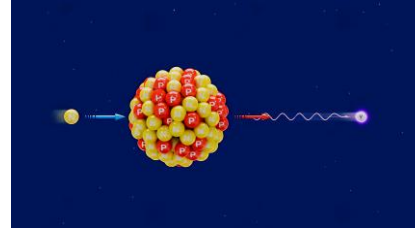
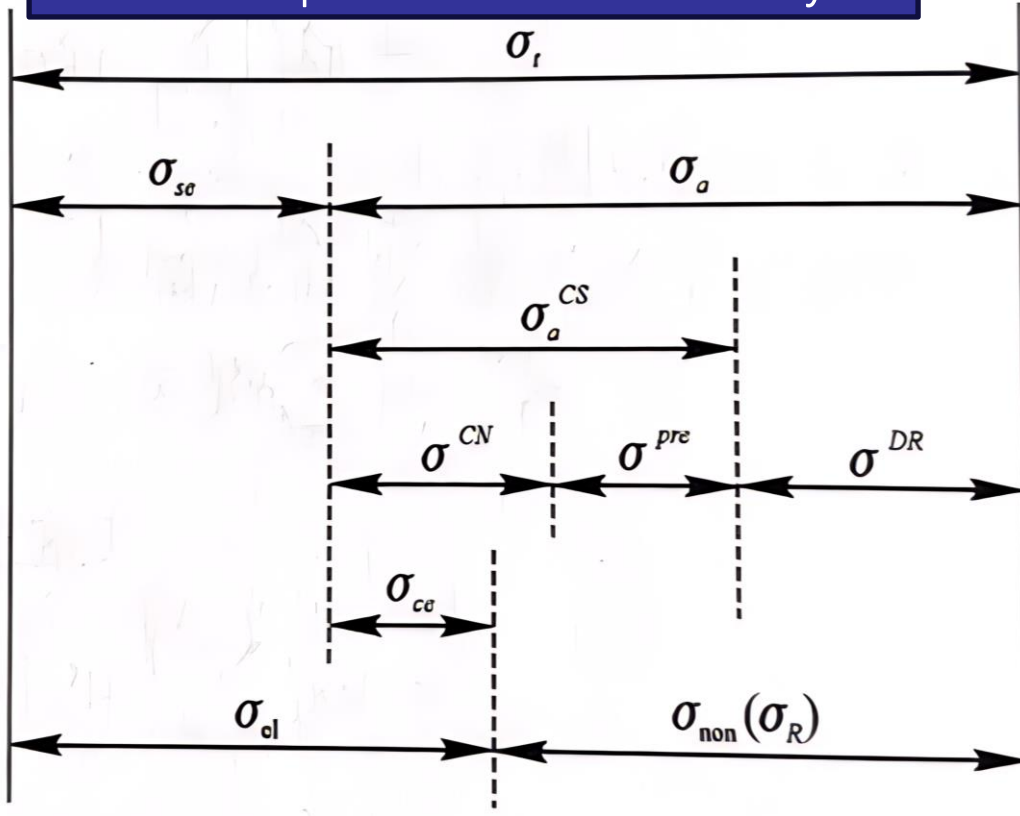
INTRODUCTION



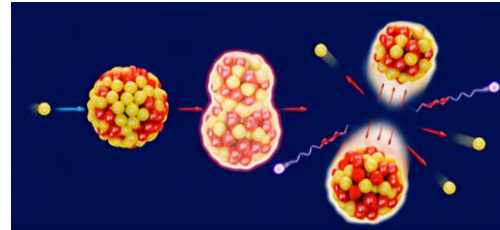
High-Precision Integrated Theoretical Platform for Neutron-Induced Reaction Data Calculations



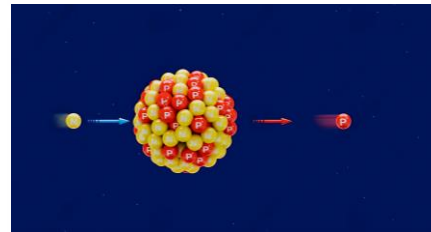
Microscopic GDR and Level Density



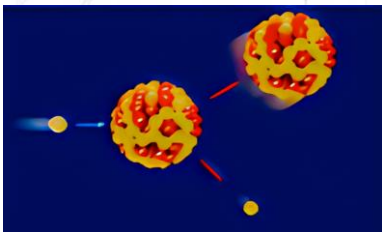
Radiative Capture Reaction
Photon Strength Function (RQRPA)
Nuclear level density (RHB)



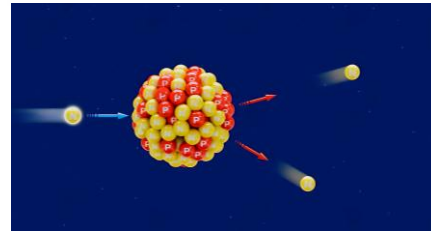
Fission Reaction
Multi-humped Fission Barrier (RHB)
Nuclear level density (RHB)



One-particle emission reactions
unified Hauser-Feshbach and
exciton model
Nuclear level density (RHB)



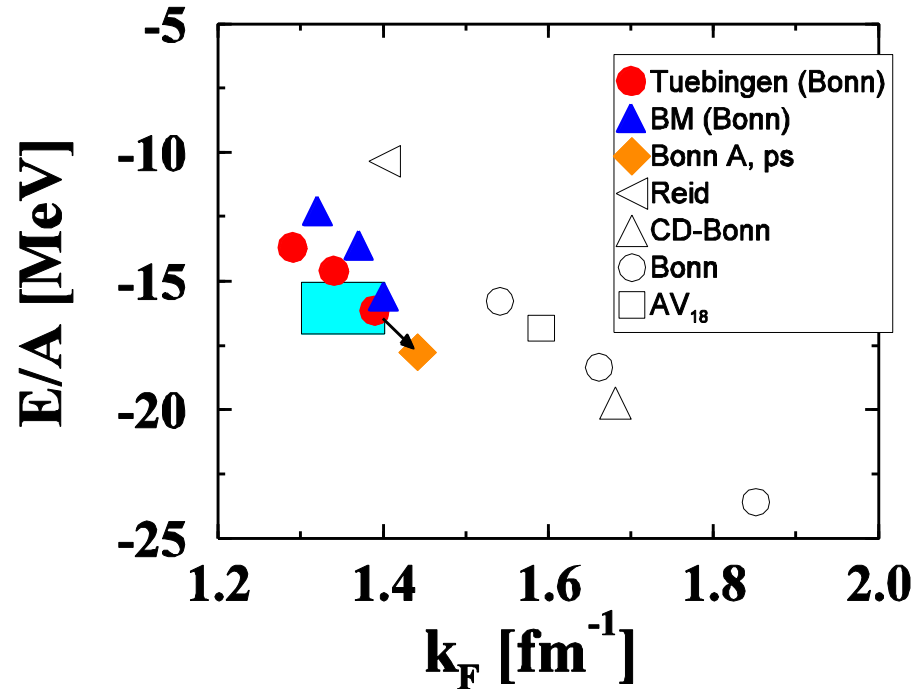
Elastic Reaction
Optical potential model
(CTOM or RHB)



Multi-particle emission reactions
Hauser-Feshbach
Nuclear level density (RHB)

Covariant density functional theory:

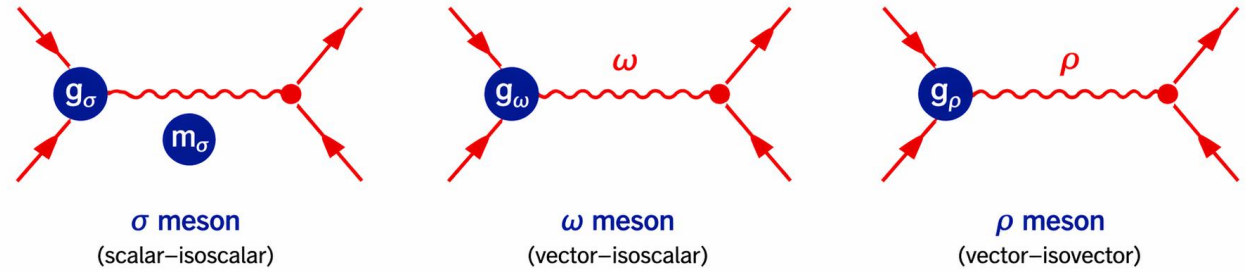
Why covariant?



C. Fuchs, LNP (2004)

Meson Exchange Interactions in Covariant Density Functional Theory

Nucleon–nucleon interaction mediated by meson exchange



- 1) Large spin-orbit splitting in nuclei
- 2) Large fields $V \approx 350$ MeV, $S \approx -400$ MeV
- 3) Success of Relativistic Brueckner
- 4) Success of intermediate energy proton scatt.
- 5) relativistic saturation mechanism
- 6) consistent treatment of time-odd fields
- 7) Pseudo-spin Symmetry
- 8) Connection to underlying theories?
- 9) As many symmetries as possible

Taken from Prof. Peter Ring's talk

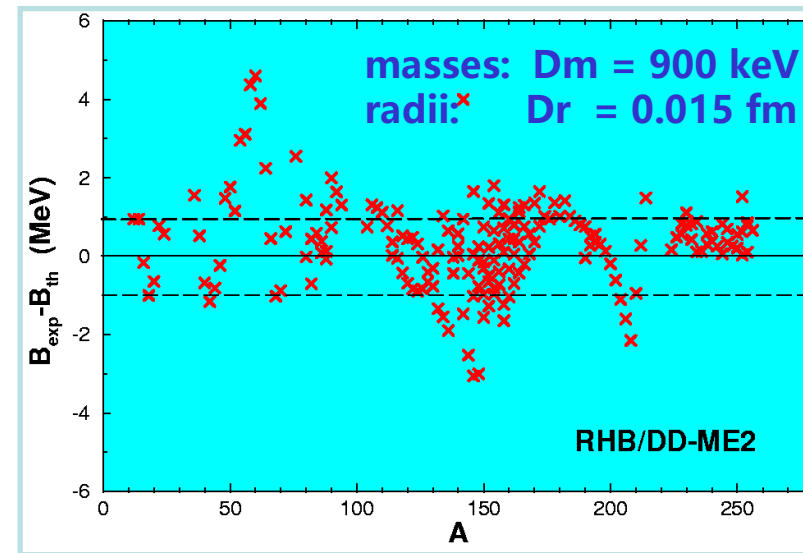
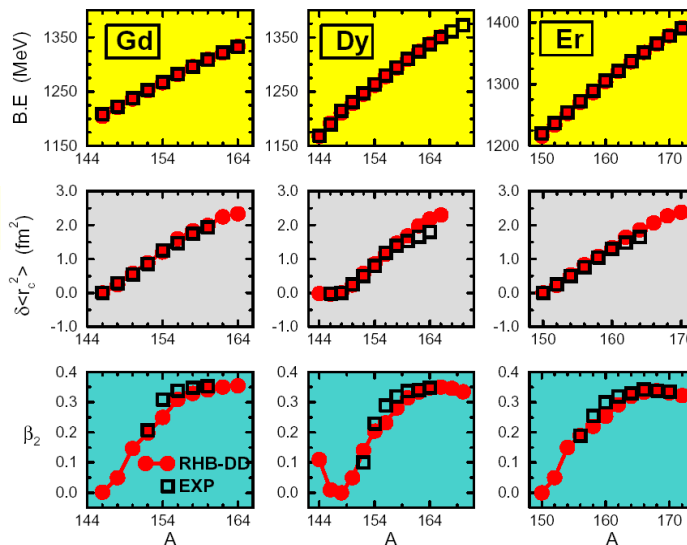
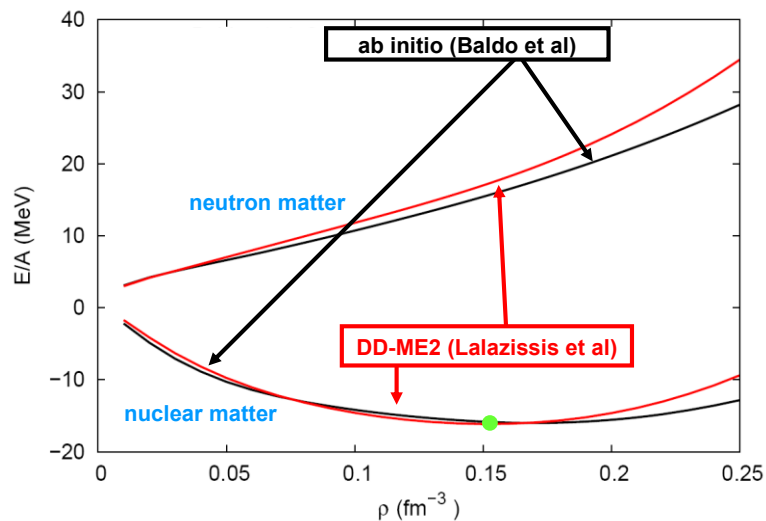
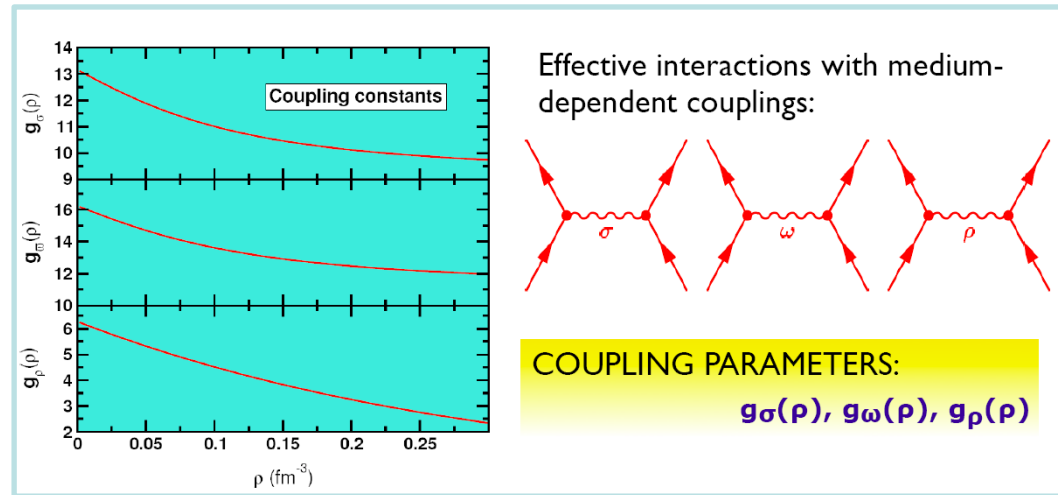
Density Dependent coupling constants:

Typel, Wolter, NPA **656**, 331 (1999)

Niksic, Vretenar, Finelli, P.R., PRC **66**, 024306 (2002): **DD-ME1**

Lalazissis, Niksic, Vretenar, P.R., PRC **78**, 034318 (2008): **DD-ME2**

	DD-ME2	DD-ME1	TW-99	NL3	NL3'
ρ_0 (fm^{-3})	0.152	0.152	0.153	0.149	0.150
E/A (MeV)	-16.14	-16.20	-16.25	-16.25	-16.31
K (MeV)	250.89	244.5	240.0	271.8	258.5
J (MeV)	32.3	33.1	32.5	37.9	38.3
m^*/m	0.572	0.578	0.556	0.60	0.595



Separable pairing interaction (TMR)

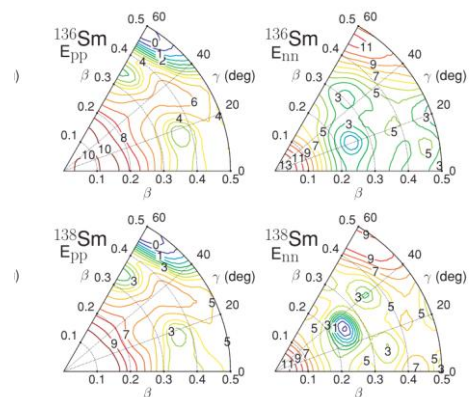
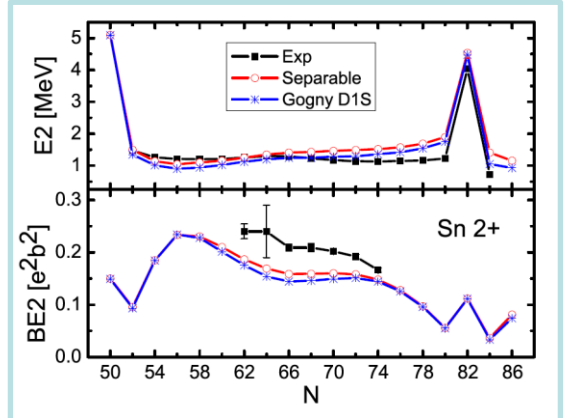
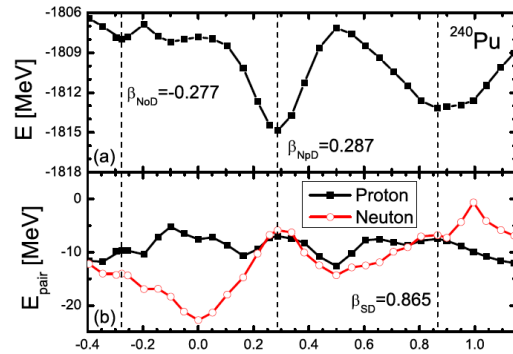
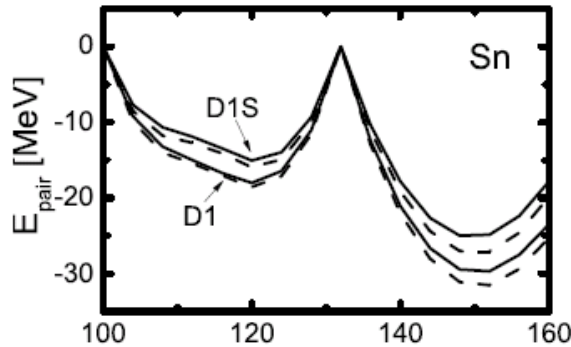
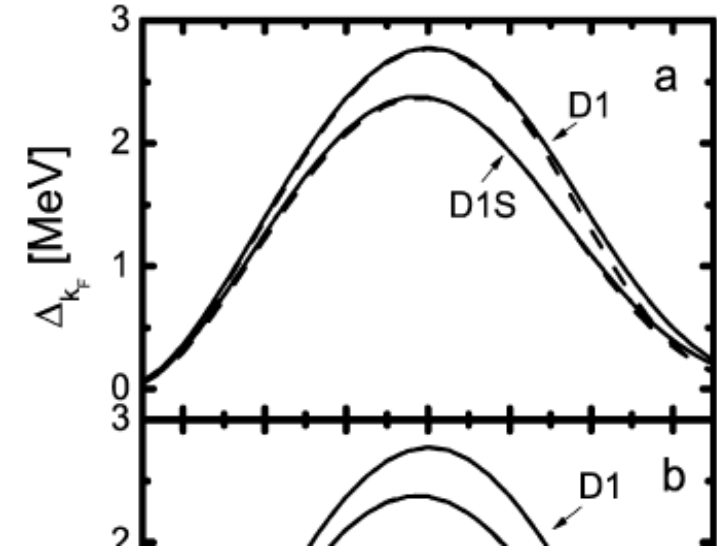
$$V_{pp}(\mathbf{r}_1\mathbf{r}_2, \mathbf{r}'_1, \mathbf{r}'_2) = -G \delta(\mathbf{R} - \mathbf{R}') e^{-(\alpha r)^2} e^{-(\alpha r')^2}$$

where $\mathbf{R} = \frac{1}{2}(\mathbf{r}_1 + \mathbf{r}_2)$,

$\mathbf{r} = \mathbf{r}_1 - \mathbf{r}_2$

$$V_{12}^0 = -G \sum_N V_{12}^N V_{1'2'}^N$$

$$V_{12}^N = M_{n_1 n_2 l}^{N 0 n_0} \frac{\hat{j}}{\hat{s} \hat{l}} \int_0^\infty R_{n0}(r, b_r) P(r) r^2 dr$$

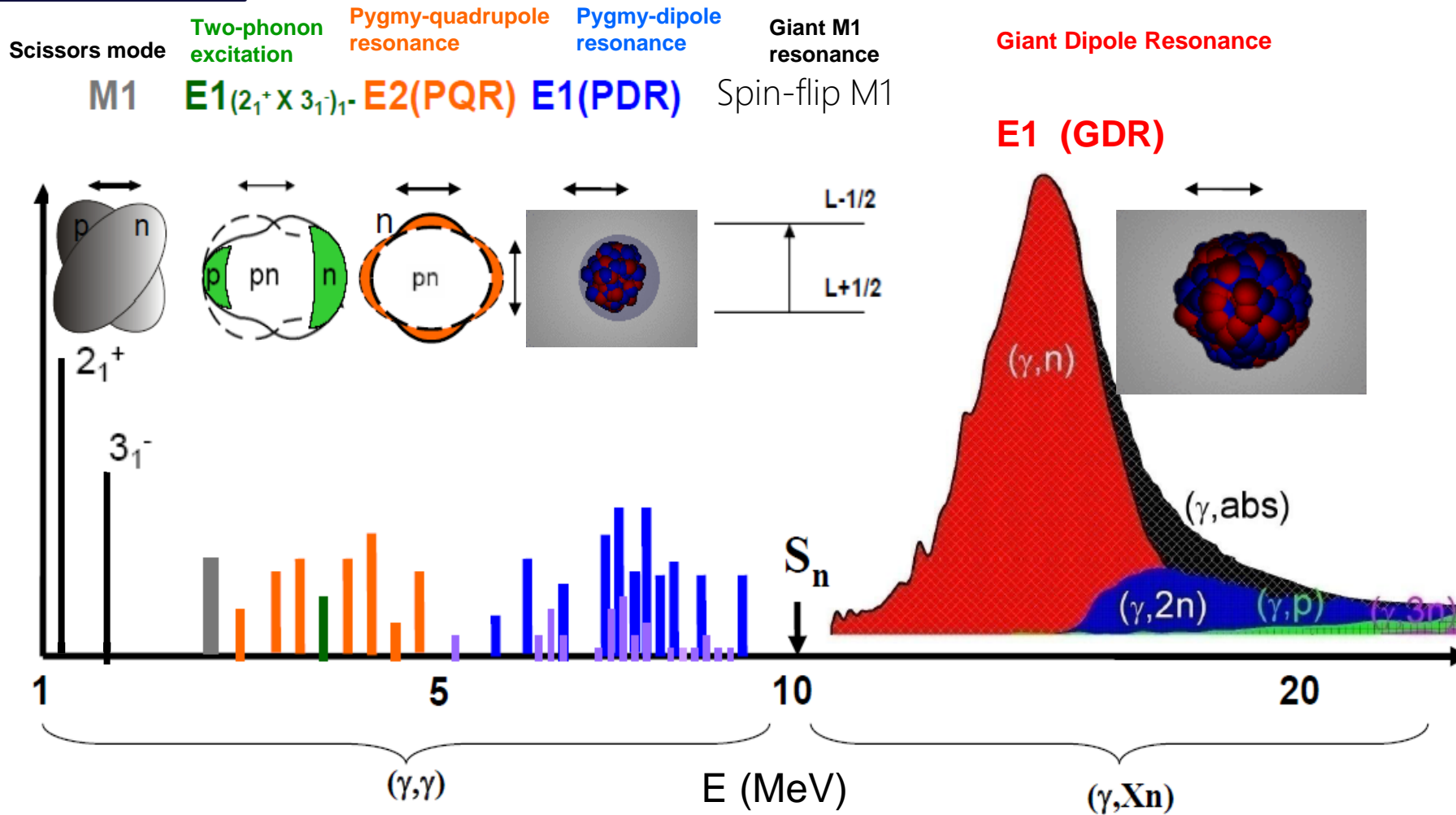


Work	Contribution	Citations
Tian, Ma & Ring PLB 676, 44 (2009)	Finite-range separable pairing force for nuclear DFT	400+
Tian, Ma & Ring PRC 80, 024313 (2009)	Axially deformed RHB calculations	100+
Tian, Ma & Ring PRC 79, 064301 (2009)	Relativistic QRPA extension	80+
Nikšić, Vretenar, Tian, Ma & Ring PRC 81, 054318 (2010)	3D/triaxial RHB calculations	120+

An aerial photograph of a park with trees in various stages of autumn, from green to bright yellow and orange. A teal banner with a white border is overlaid in the center, containing the text "Giant Dipole Resonance".

Giant Dipole Resonance

Radiative Capture Reaction



Moderate and Heavy nuclei

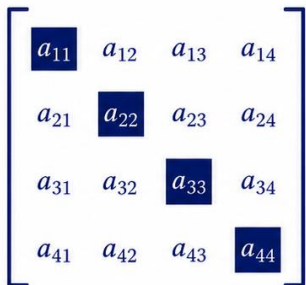
Theoretical prediction of Pygmy Quadrupole Resonance: N. Tsoneva, H. Lenske, Phys. Lett. B 695 (2011) 174.

N.Tsoneva, ERICE14

RQRPA: using the diagonalization approach

$$\begin{pmatrix} A^J & B^J \\ B^{*J} & A^{*J} \end{pmatrix} \begin{pmatrix} X^{\nu, JM} \\ Y^{\nu, JM} \end{pmatrix} = \omega_{\nu} \begin{pmatrix} 1 & 0 \\ 0 & -1 \end{pmatrix} \begin{pmatrix} X^{\nu, JM} \\ Y^{\nu, JM} \end{pmatrix}$$

Small Matrix

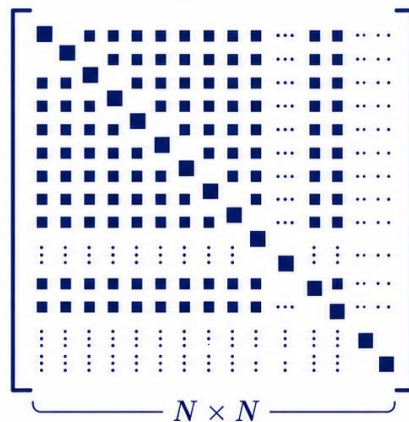


Direct Diagonalization
 $Ax = \lambda x$

Computational cost $\sim O(N^3)$
Memory cost $\sim O(N^2)$

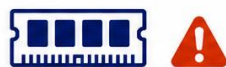
Small dimension, can be diagonalized directly

Large Matrix



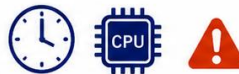
Huge dimension, memory and computation time grow rapidly

Memory Bottleneck



Memory cost $\sim O(N^2)$
Memory demand quickly exceeds available capacity

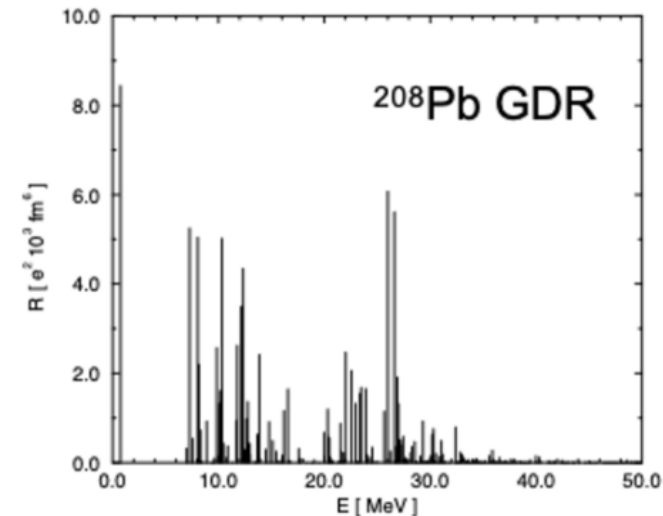
Time Bottleneck



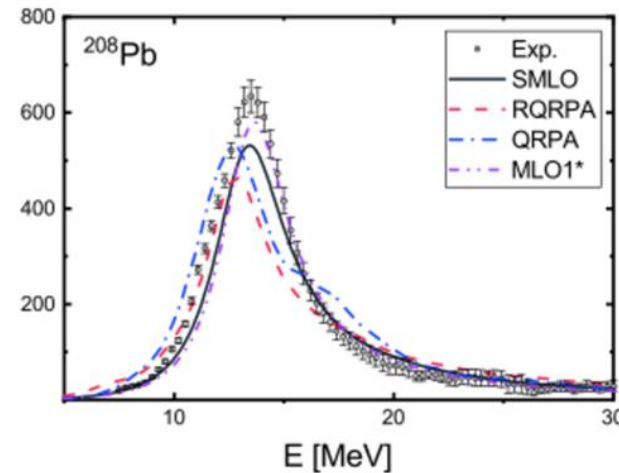
Computational cost $\sim O(N^3)$
Runtime increases dramatically making completion within a reasonable time difficult

When the matrix dimension becomes very large, direct diagonalization becomes extremely difficult

Example: spherical QRPA $\sim 3 \times 10^3$, manageable; deformed QRPA $\sim 10^5$, direct diagonalization is extremely expensive



requires the introduction of a width to obtain the excitation curve



RQRPA: for the spherical nuclei

Chinese Physics C Vol. 43, No. 11 (2019) 114102

Giant dipole resonance parameters from photoabsorption cross-sections*

Yuan Tian(田源)^{1,3} Xi Tao(陶曦)¹ Jimin Wang(王记民)¹ Xianbo Ke(柯贤博)^{1,2}
Ruirui Xu(续瑞瑞)^{1,2,3} Zhigang Ge(葛智刚)¹

¹China Nuclear Data Center, China Institute of Atomic Energy, P.O. Box 275(41), Beijing 102413, China
²Guangxi Normal University, Guilin, Guangxi Province, 541004, China

$$\sigma_{E1}(\epsilon_\gamma) = \frac{16\pi^3 e^2}{9 \hbar c} G\epsilon_\gamma S_{E1}(\epsilon_\gamma)$$

$$S_{E1}(\epsilon_\gamma) = \sum_\nu \frac{B(1, \omega_\nu)}{\pi} \frac{\Gamma(\epsilon_\gamma)/2}{(\epsilon_\gamma - \omega_\nu)^2 + (\Gamma(\epsilon_\gamma)/2)^2}$$

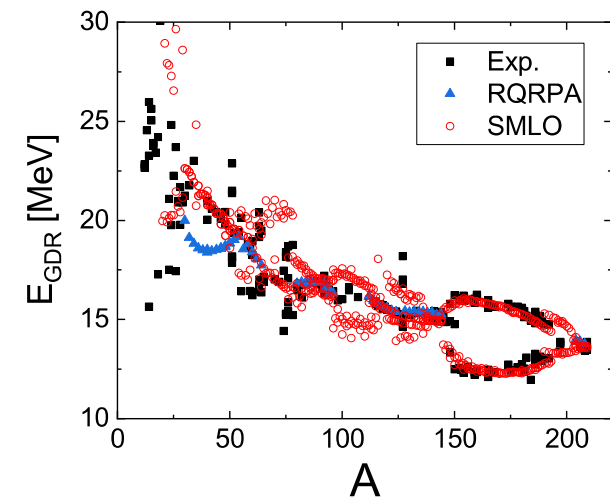
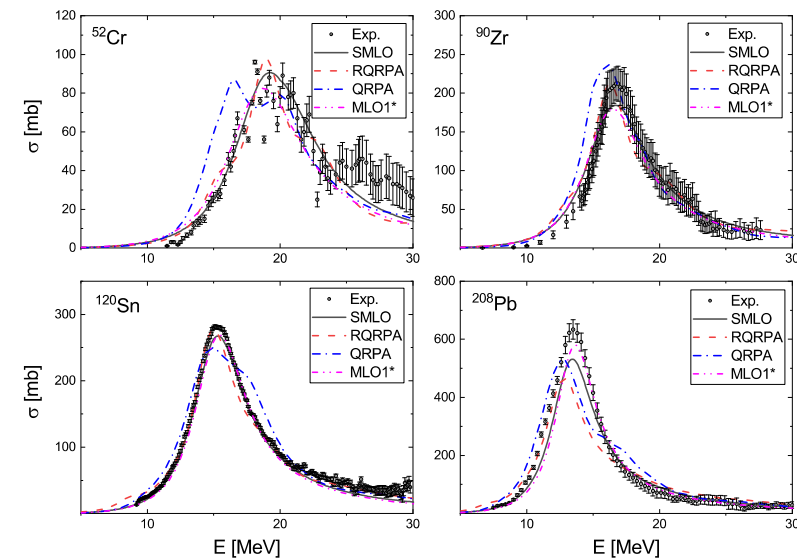
$$\Gamma(\epsilon_\gamma) = \Gamma \sqrt{\epsilon_\gamma/E_{E1}}$$

TABLE III. The parameters and χ_{tot}^2 of microscopic GDR parameters within RQRPA. C means constant width of the Lorentzian distribution., ED stands for energy-dependent width.

	Γ	G	χ_{tot}^2
RQRPA	2.0 (C)	1.0	270.0
RQRPA(fitted)	1.59 (ED)	0.65	21.0

TABLE I. Experimental value of the spherical nuclei we use to fit the systematic GDR parameters.

Nucleus	points	Energy range [MeV]	Ref.	def.	β_2
³⁴ S	29	12.0 - 26.0	[28]		0.00
⁴⁰ Ar	61	10.0 - 40.0	[29]		0.00
⁴⁰ Ca	70	11.25 - 28.1	[30]		0.00
⁴² Ca	151	10.0 - 40.0	[31]		0.00
⁴⁴ Ca	58	11.5 - 40.0	[31]		0.00
⁴⁸ Ca	60	10.5 - 40.0	[31]		0.00
⁴⁸ Ti	58	11.5 - 40.0	[31]		0.00
⁵¹ V	41	10.47 - 32.69	[32]		0.00
⁵² Cr	115	11.5 - 40.0	[29]		0.00
⁹⁰ Zr	46	12.2 - 25.7	[33]		0.035
⁹¹ Zr	101	10.8 - 30.0	[34]		0.053
⁹² Zr	105	15.8 - 27.8	[35]		0.053
⁹⁴ Zr	92	7.85 - 31.0	[34]		0.063
¹¹² Sn	167	10.9 - 27.5	[36]		0.018
¹¹⁴ Sn	168	10.4 - 27.1	[36]		0.00
¹¹⁶ Sn	200	9.70 - 29.6	[36]		0.00
¹¹⁷ Sn	232	7.40 - 30.9	[36]		-0.044
¹¹⁸ Sn	211	9.40 - 30.7	[36]		0.00
¹¹⁹ Sn	233	7.40 - 31.1	[36]		0.00
¹²⁰ Sn	207	9.20 - 29.8	[36]		0.00
¹²² Sn	184	8.90 - 27.2	[36]		0.00
¹²⁴ Sn	220	8.60 - 30.9	[36]		0.00
¹³⁸ Ba	61	8.48 - 27.1	[37]		0.00
²⁰⁸ Pb	101	7.50 - 37.5	[38]		0.00
²⁰⁹ Bi	109	8.01 - 26.4	[37]		-0.008



FAM solves the linear response equations through a self-consistent iterative approach


$$\begin{aligned}
 (E_\mu + E_\nu - \omega_\gamma) X_{\mu\nu}(\omega_\gamma) &= - \left(F_{\mu\nu}^{20}(\omega_\gamma) + \delta H_{\mu\nu}^{20}(\omega_\gamma) \right), \\
 (E_\mu + E_\nu + \omega_\gamma) Y_{\mu\nu}(\omega_\gamma) &= - \left(F_{\mu\nu}^{02}(\omega_\gamma) + \delta H_{\mu\nu}^{02}(\omega_\gamma) \right),
 \end{aligned}$$

$$\begin{aligned}
 \delta H_{\mu\nu}^{20}(\omega) &= \sum_{\mu' < \nu'} \{ A_{\mu\nu, \mu'\nu'} - (E_\mu + E_\nu) \delta_{\mu\mu'} \delta_{\nu\nu'} \} X_{\mu'\nu'}(\omega) \\
 &\quad + \sum_{\mu' < \nu'} B_{\mu\nu, \mu'\nu'} Y_{\mu'\nu'}(\omega) \\
 \delta H_{\mu\nu}^{02}(\omega) &= \sum_{\mu' < \nu'} \{ A_{\mu\nu, \mu'\nu'}^* - (E_\mu + E_\nu) \delta_{\mu\mu'} \delta_{\nu\nu'} \} X_{\mu'\nu'}(\omega) \\
 &\quad + \sum_{\mu' < \nu'} B_{\mu\nu, \mu'\nu'}^* Y_{\mu'\nu'}(\omega)
 \end{aligned}$$

$$\left[\begin{pmatrix} A & B \\ B^* & A^* \end{pmatrix} - \omega \begin{pmatrix} 1 & 0 \\ 0 & -1 \end{pmatrix} \right] \begin{pmatrix} X(\omega) \\ Y(\omega) \end{pmatrix} = - \begin{pmatrix} F^{20} \\ F^{02} \end{pmatrix}$$

Restricting calculations to fixed-size widths makes it difficult to reproduce experimental data


Computer Physics Communications 253 (2020) 107184



Contents lists available at [ScienceDirect](#)

Computer Physics Communications


journal homepage: www.elsevier.com/locate/cpc



Implementation of the quasiparticle **finite amplitude method** within the relativistic self-consistent mean-field framework: The program DIRQFAM ^{☆, ☆☆}

A. Bjelčić, T. Nikšić*
 University of Zagreb, Faculty of Science, Physics Department, Croatia

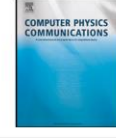
Computer Physics Communications 287 (2023) 108689



Contents lists available at [ScienceDirect](#)

Computer Physics Communications

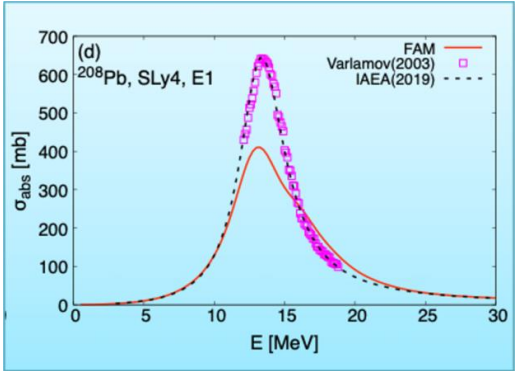
journal homepage: www.elsevier.com/locate/cpc



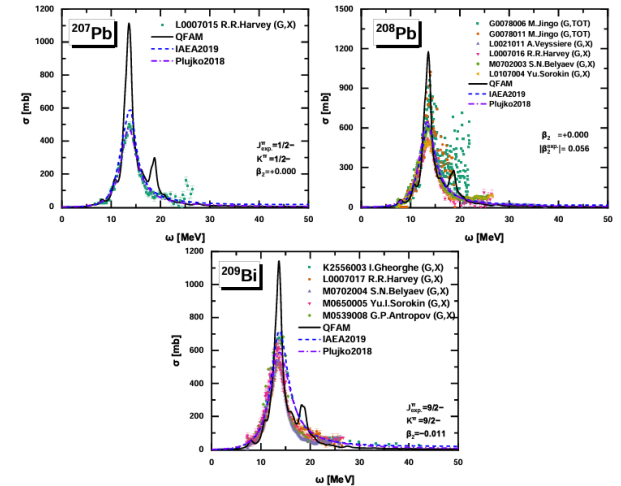
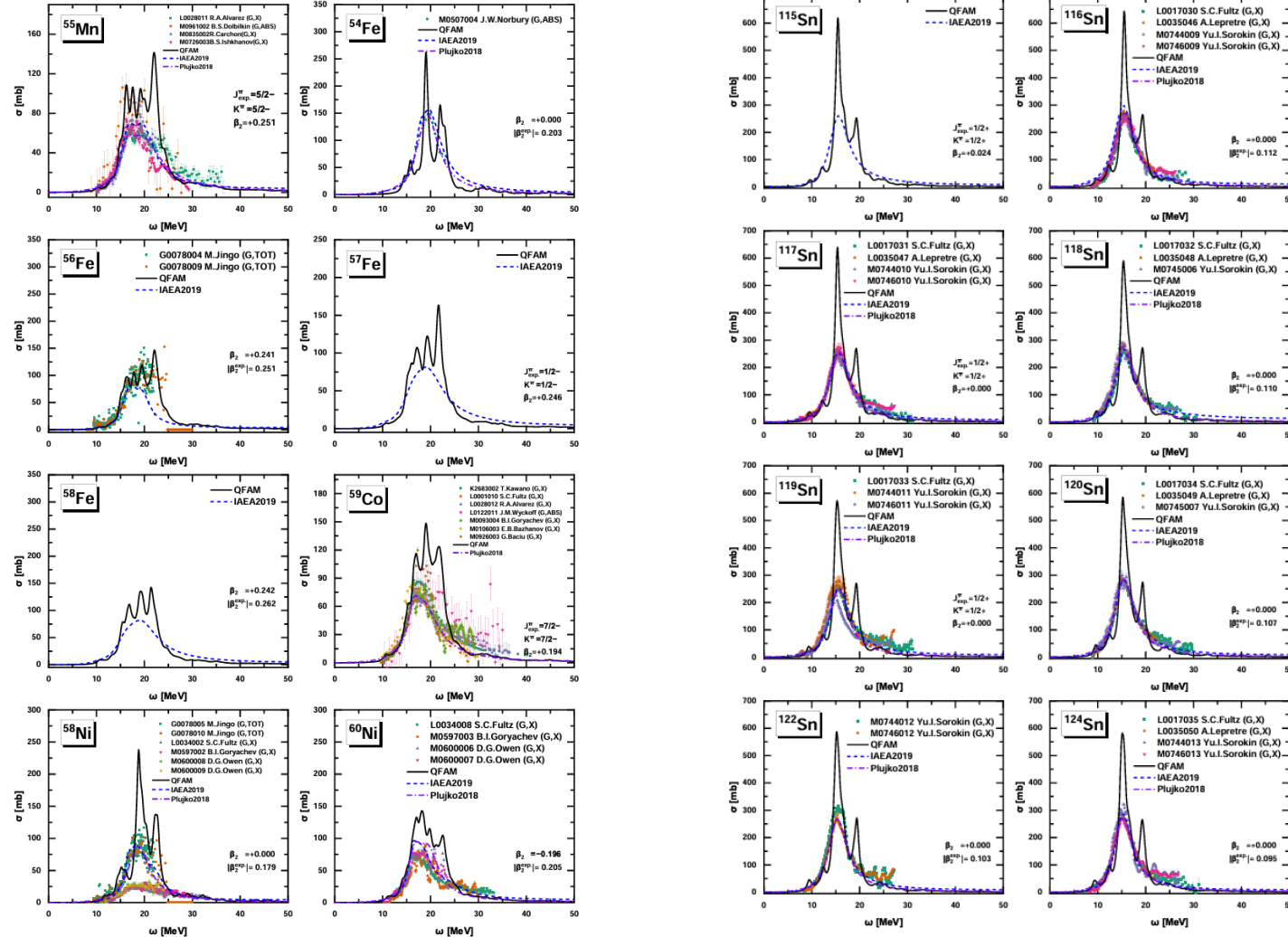
Implementation of the quasiparticle finite amplitude method within the relativistic self-consistent mean-field framework (II): The program DIRQFAM v2.0.0 ^{☆, ☆☆}

A. Bjelčić, T. Nikšić*

N_{shells}	Memory [GB]	Time [s]
10	0.42 (0.75)	0.24 (0.36)
12	0.68 (1.46)	0.49 (0.82)
14	1.11 (2.75)	0.99 (1.75)
16	1.77 (5.68)	1.82 (3.32)
18	2.83 (8.39)	3.23 (5.71)
20	4.40 (13.9)	5.52 (9.54)
22	6.65 (22.2)	8.97 (15.5)
24	11.1 (34.2)	14.1 (26.0)



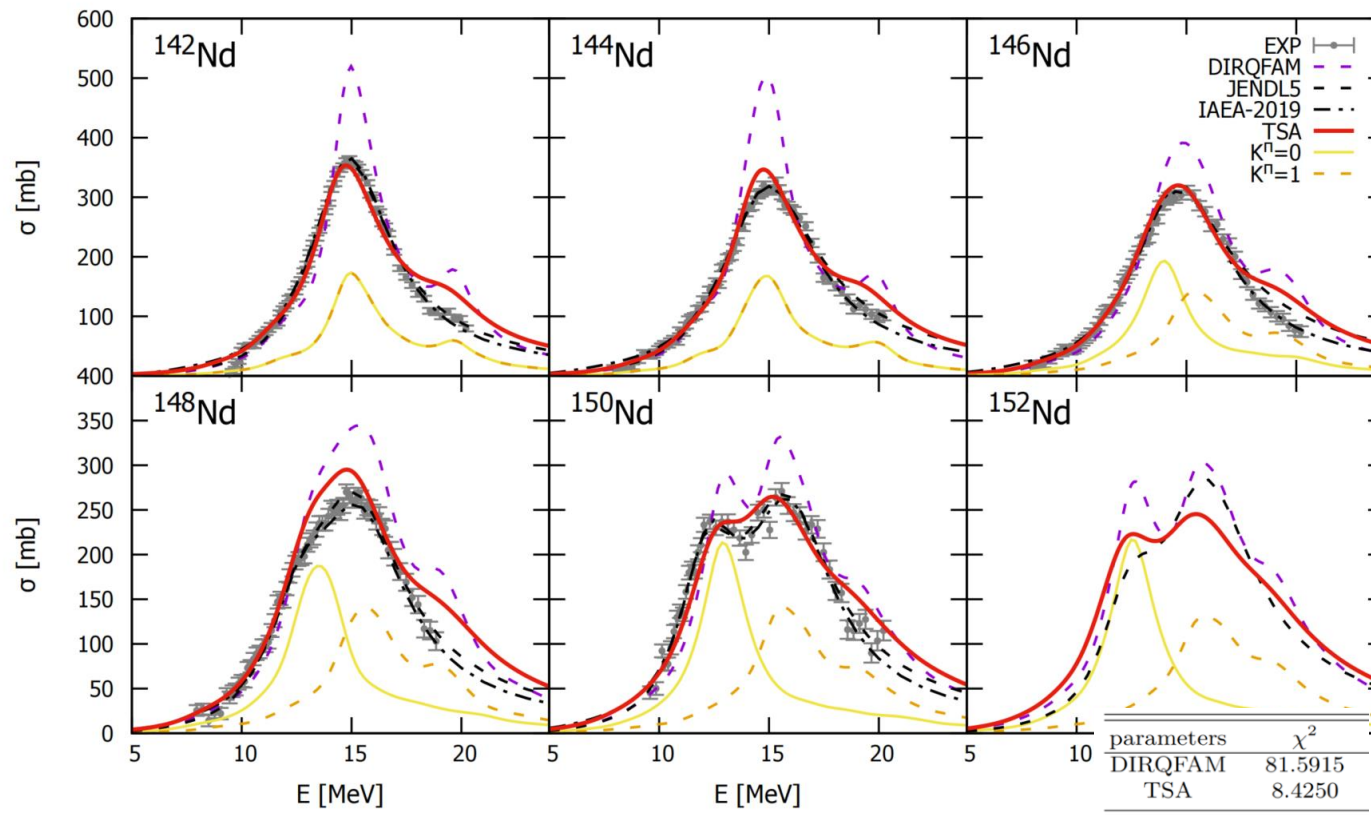
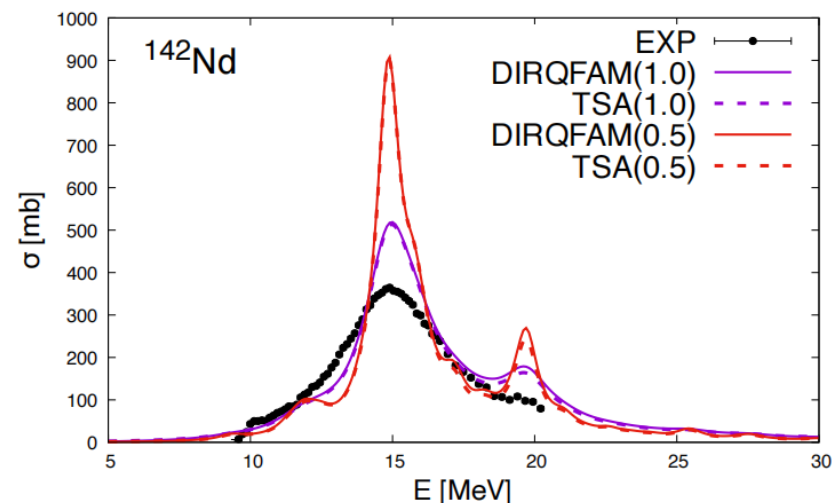
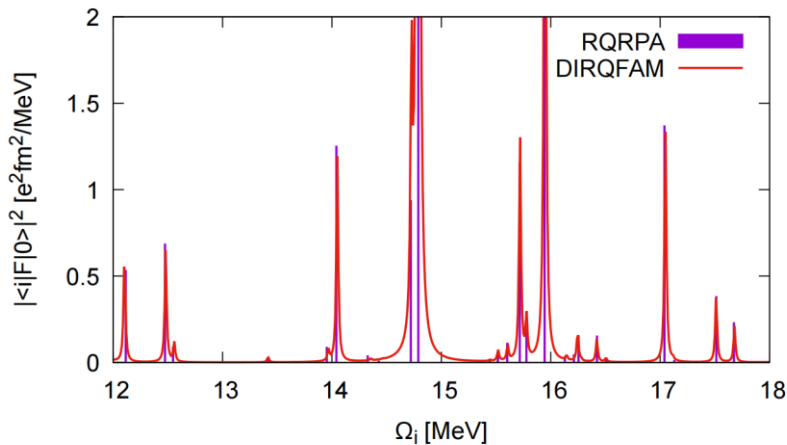
Radiative Capture Reaction



Photoabsorption cross sections for 235 stable nuclei, ranging from ^{40}Ca to ^{209}Bi , were investigated by the quasiparticle finite amplitude method (QFAM) using relativistic pion coupling interaction DD-PC1, with extensions to odd-A nuclei.

Atomic Data and Nuclear Data Tables
Volume 168, February 2026, 101770

Energy-dependent width improves QFAM description of GDR



This paper investigates the photon absorption cross-sections of even-even nuclei within the Nd isotope chain. By fitting energy-dependent widths, the deviation between the original QFAM results and experimental values was reduced by an order of magnitude;

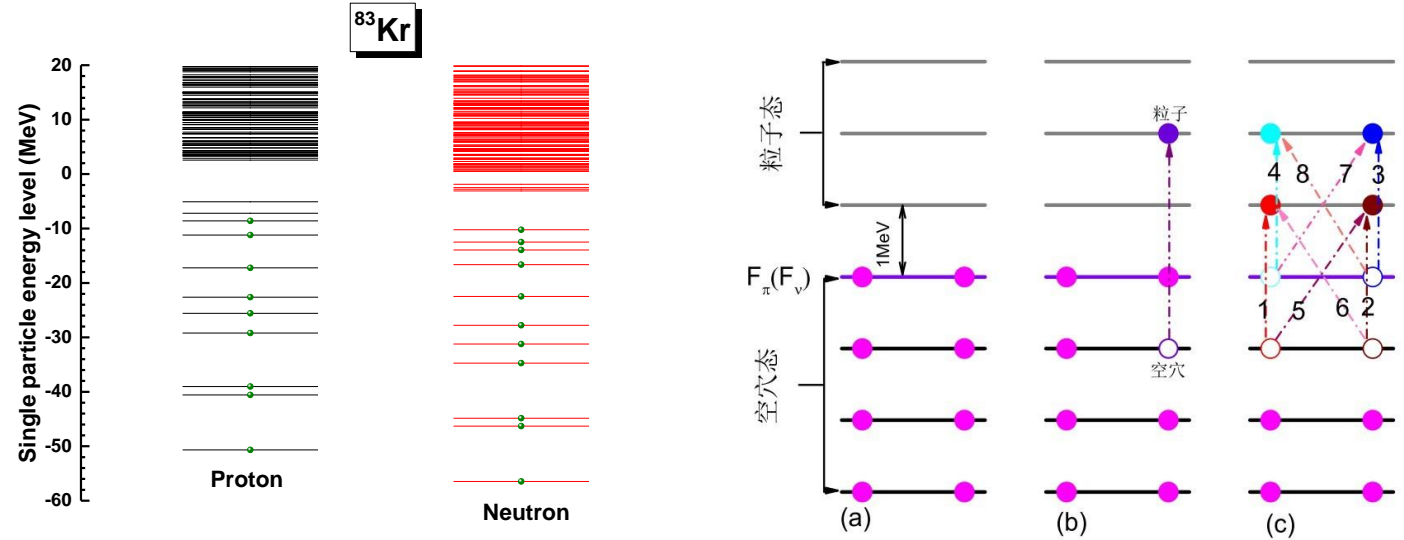
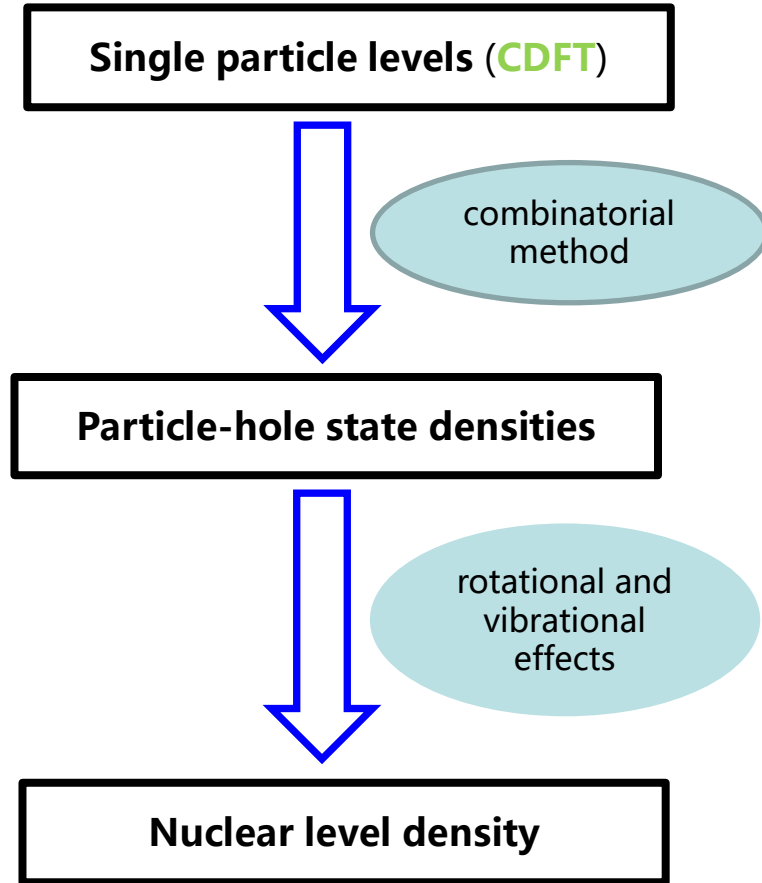
Nuclear Science and Techniques (2025) 36:241



Nuclear Level Densities



Microscopic nuclear level densities based on CDFT



$$\rho_{sph}(U, J, P) = \omega_i(U, M = J, P) - \omega_i(U, M = J + 1, P)$$

$$\rho_{def}(U, J, P) = 1/2[\sum_{K=-J, K \neq 0}^J \omega_i(U - E_{rot}^{J,K}, K, P)] + \delta_{(J_{even})} \delta_{(P=+)} \omega_i(U - E_{rot}^{J,0}, 0, P) + \delta_{(J_{odd})} \delta_{(P=-)} \omega_i(U - E_{rot}^{J,0}, 0, P)$$

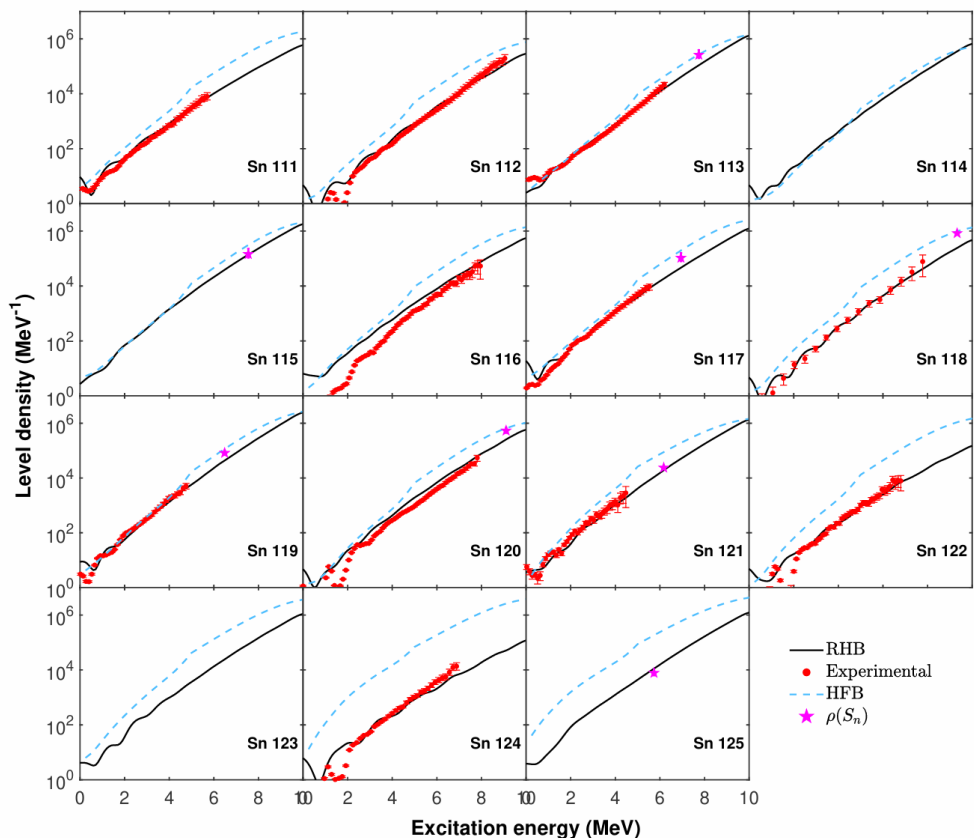
Global microscopic nuclear level densities within the HFB\ plus combinatorial method for practical applications

Hilaire, S. / Goriely, S. 2006 *Nuclear Physics A*, Vol. 779 p. 63 - 81

Chinese Physics C Vol. 50, No. 5 (2026) 054107

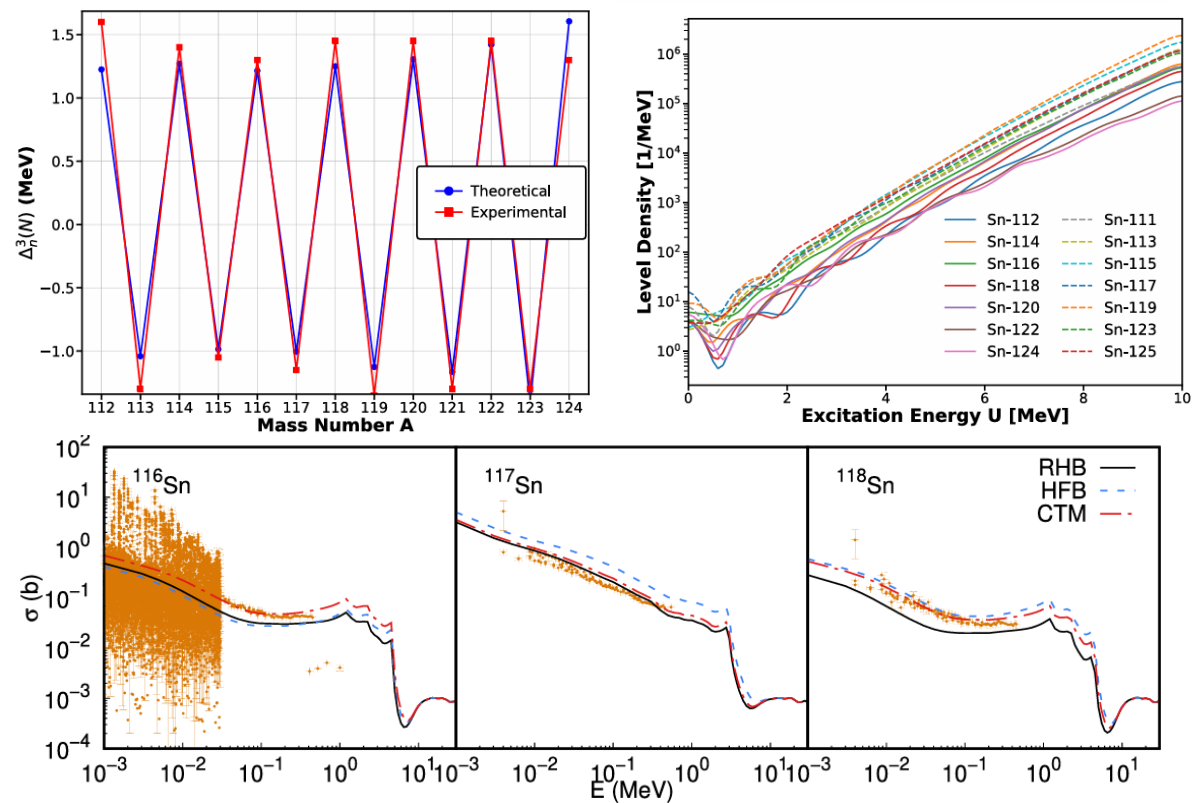
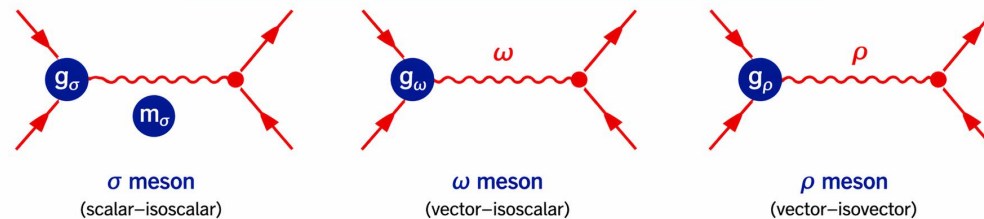
Systematic study of microscopic nuclear level densities of Sn isotopes within a relativistic framework*

Guanbin He (何冠彬)¹ Nuocheng Tang (唐诺程)¹ Yuan Tian (田源)^{1†} Ying Cui (崔莹)¹
Jian Li (李剑)² Yi Xu (徐毅)^{1,3†} Ruirui Xu (续瑞瑞)^{1,8}



Meson Exchange Interactions in Covariant Density Functional Theory

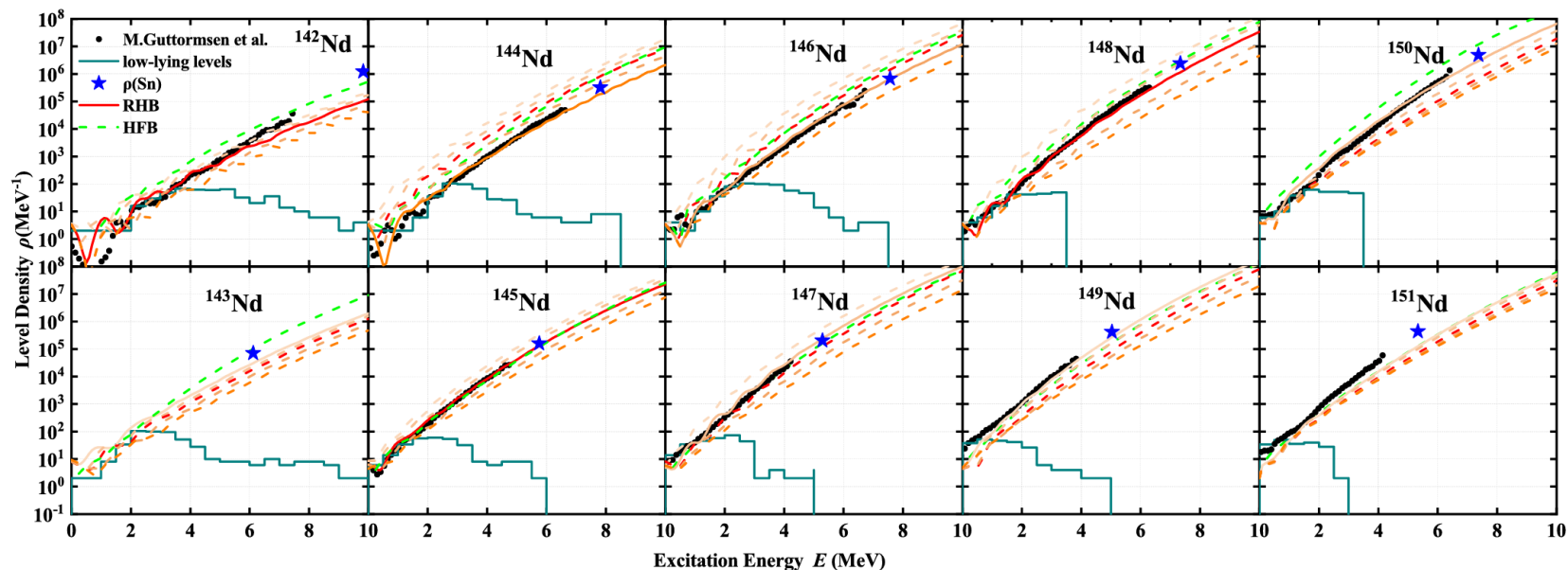
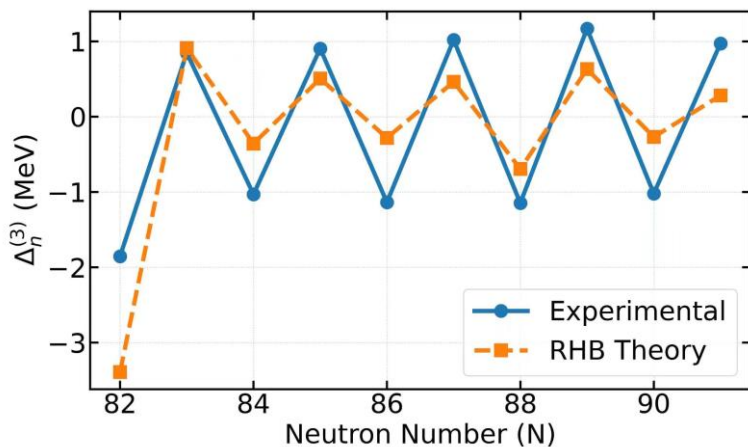
Nucleon–nucleon interaction mediated by meson exchange



Pairing effect on the Microscopic Level Density

Pairing sensitivity:

The default pairing strength tends to underestimate pairing correlations in Nd isotopes. By scaling the pairing strength from 0.8 to 1.2, we find that microscopic level densities are **strongly correlated with pairing correlations**, especially in the low-excitation-energy region. This indicates that pairing optimization is essential for reliable microscopic NLD predictions.



In preparation

FIG. 3. Microscopic level densities of $^{142-151}\text{Nd}$ calculated with different values of the pairing scaling factor λ . The recommended result selected from the D_0 constraint and auxiliary Oslo comparison is highlighted. The low-lying discrete levels, available Oslo-type level densities, and neutron-resonance constraint at S_n are shown for comparison.

RQRPA + Boson expansion

A new approach to nuclear level densities: The QRPA plus boson expansion



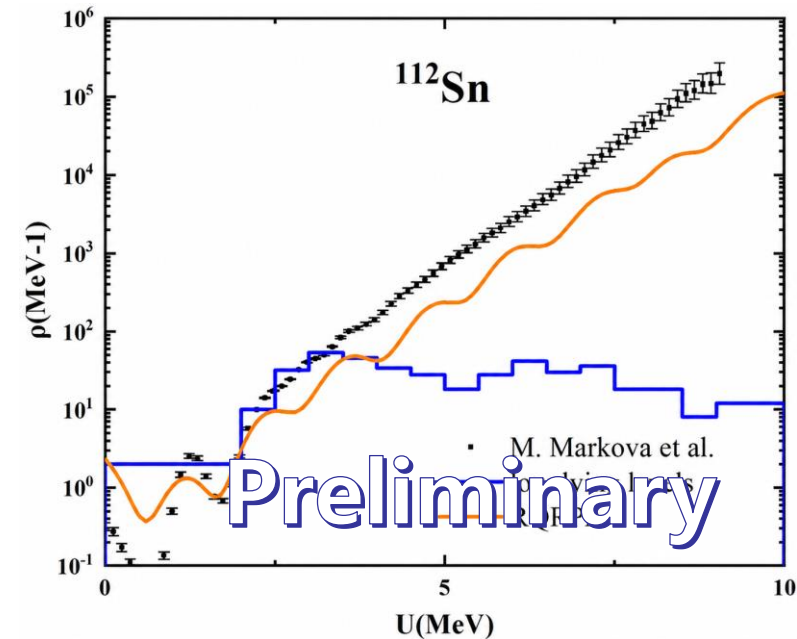
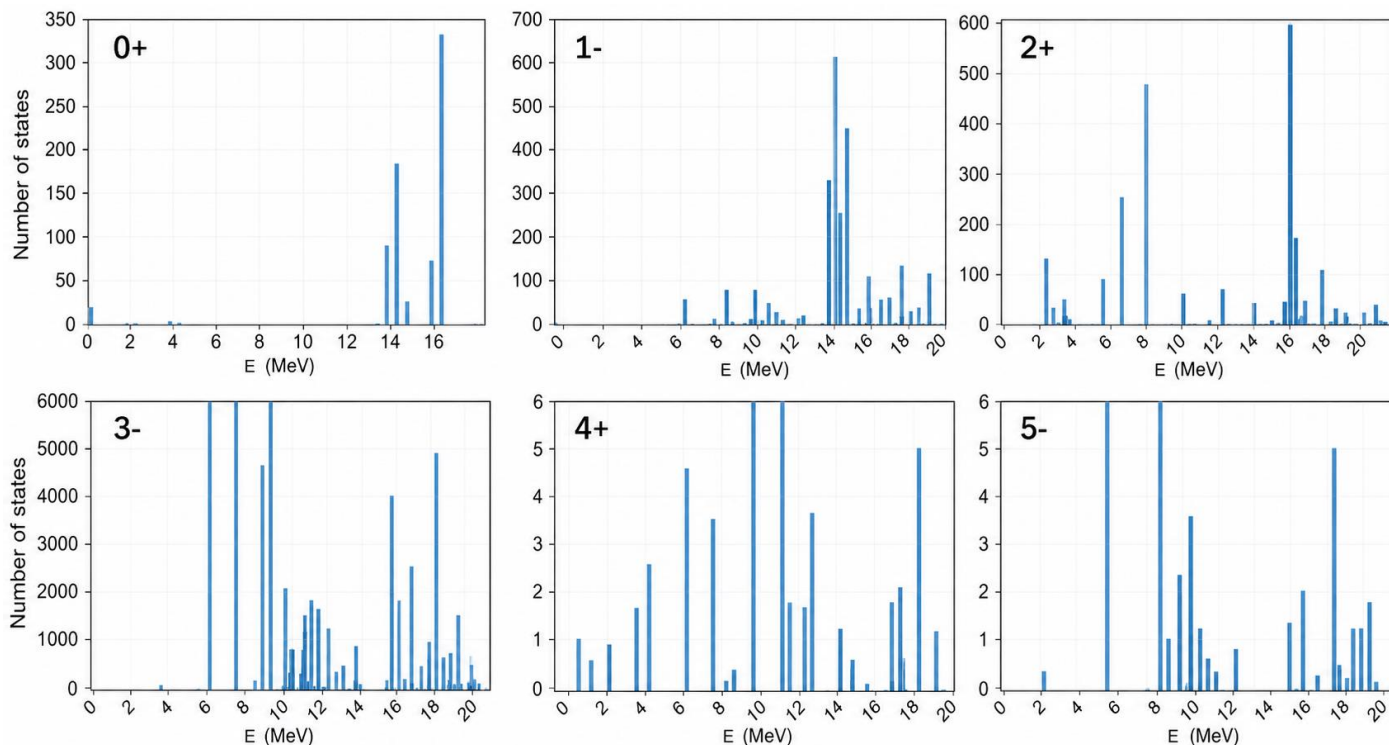
S. Hilaire^{a,b,*}, S. Goriely^c, S. Péru^{a,b}, G. Gosselin^{a,b}

Physics Letters B 843 (2023) 137989

^a CEA, DAM, DIF, F-91297 Arpajon, France

^b Université Paris-Saclay, CEA, LMCE, 91680 Bruyères-le-Châtel, France

^c Institut d'Astronomie et d'Astrophysique, Université Libre de Bruxelles, Campus de la Plaine CP 226, 1050 Brussels, Belgium



Current status and next step

- The present boson-expansion space is constructed from **electric** RQRPA phonons.
- **Magnetic** phonons, are not included. 1^+M1 excitations, are included by experiment data.
- Deformed nuclei need to be calculated with **DIRQFAM**.

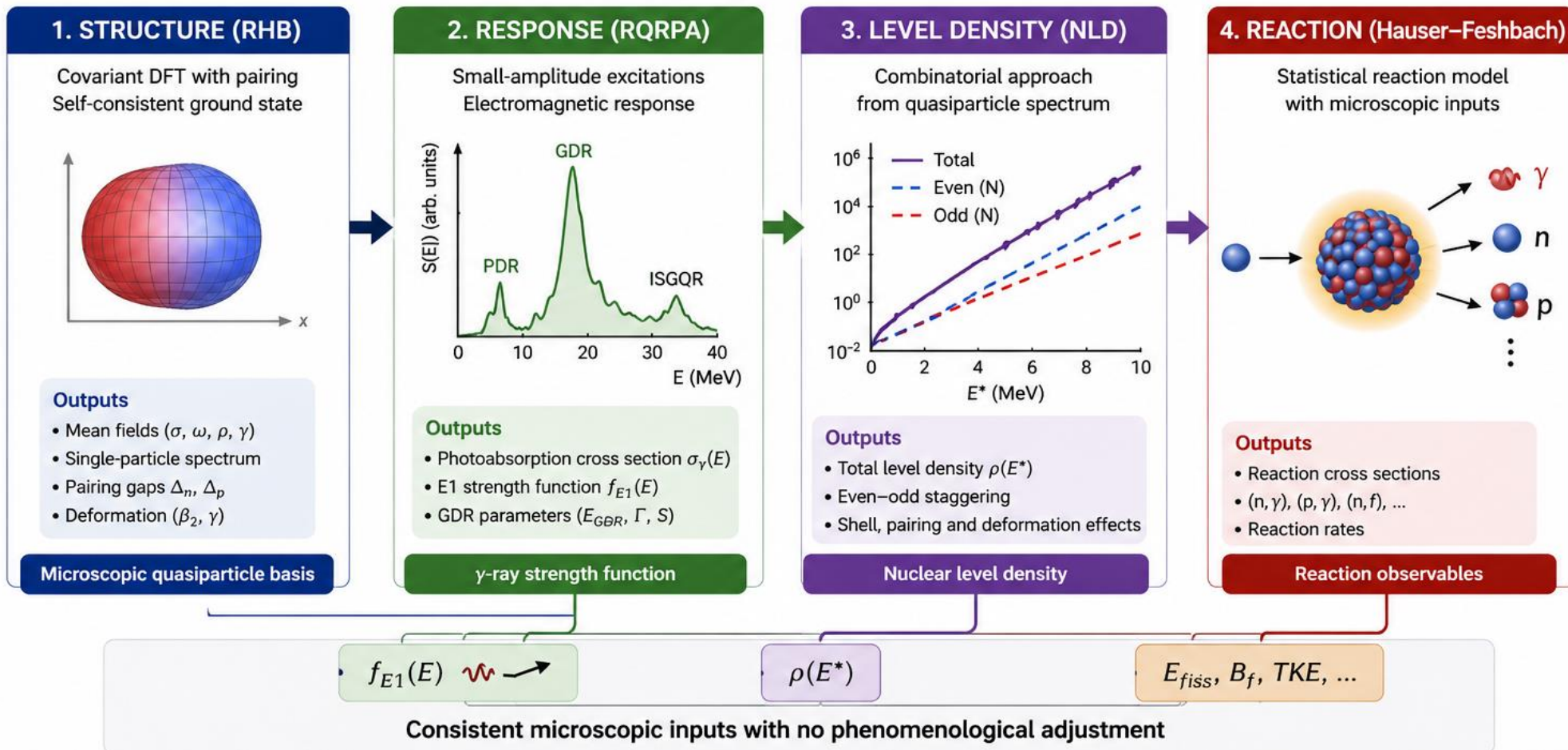


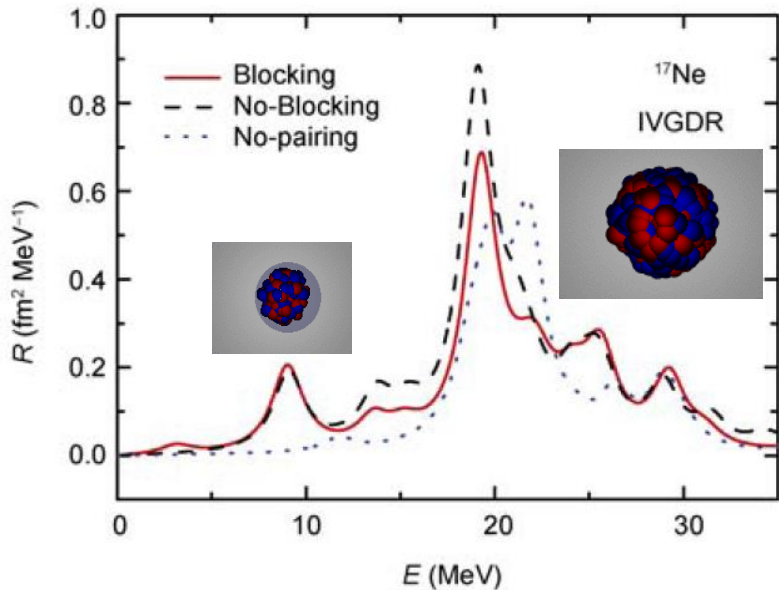
CONCLUSION AND OUTLOOK



A Unified Microscopic Framework: Structure → Response → Reaction

From covariant energy density functional theory to nuclear observables

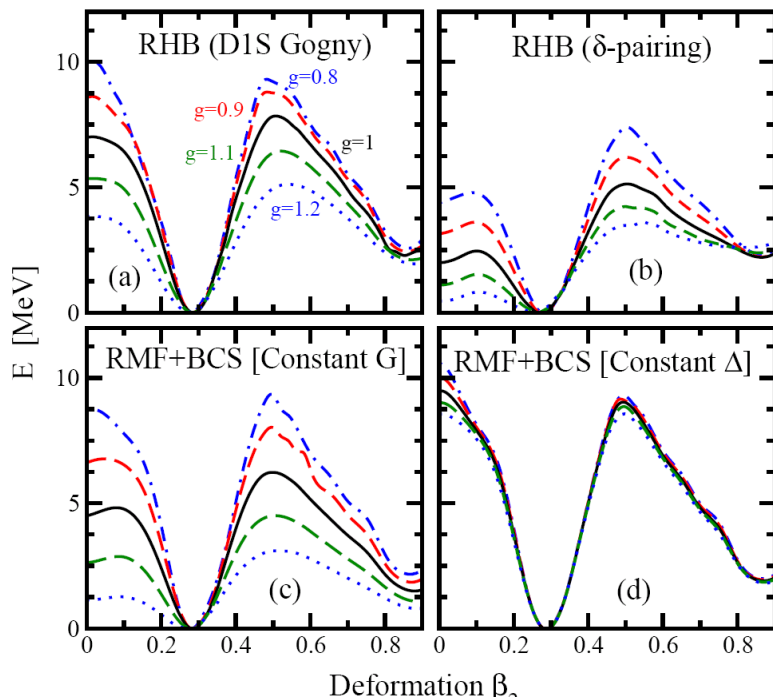




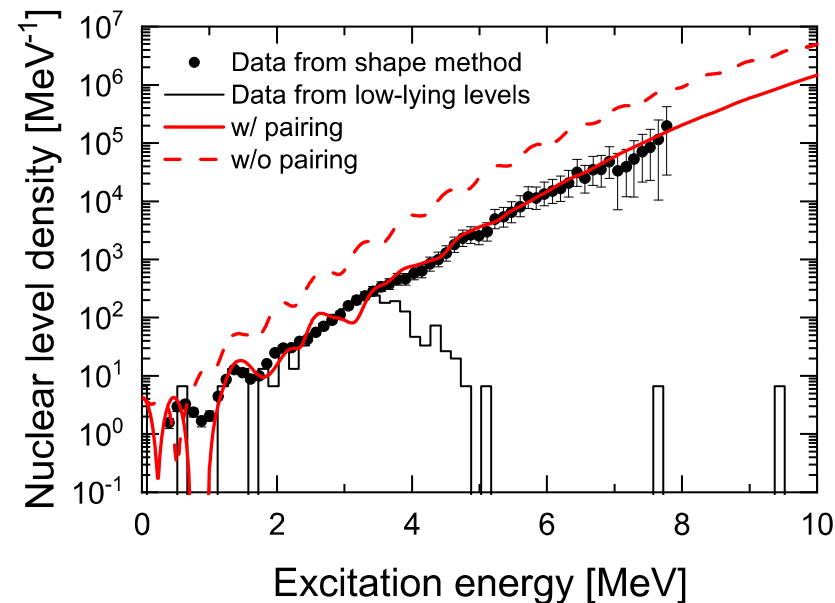
SCIENCE CHINA
Physics, Mechanics & Astronomy

• Research Paper •
Radioactive Nuclear Beam Physics and Nuclear Astrophysics

August 2011, Vol.54, Suppl. 1: s49–s52
doi: 10.1007/s11433-011-4416-8



Physics Letters B 689 (2010) 72–8



Phys. Lett. B 849 (2024) 138448

A self-consistent microscopic treatment of pairing correlations in finite nuclei is essential for improving predictions of giant dipole resonances, fission barriers, and nuclear level densities.



Thank you for your attention!

Physics Letters B 753 (2016) 13–17



ELSEVIER

Contents lists available at ScienceDirect

Physics Letters B

www.elsevier.com/locate/physletb



Stochastic estimation of nuclear level density in the nuclear shell model: An application to parity-dependent level density in ^{58}Ni

Noritaka Shimizu^{a,*}, Yutaka Utsuno^{a,b}, Yasunori Futamura^c, Tetsuya Sakurai^{c,d}, Takahiro Mizusaki^e, Takaharu Otsuka^{a,f,g,h}

^a Center for Nuclear Study, the University of Tokyo, Hongo, Tokyo, 113-0033, Japan

^b Advanced Science Research Center, Japan Atomic Energy Agency, Tokai, Ibaraki 319-1195, Japan

^c Faculty of Engineering, Information and Systems, University of Tsukuba, Tsukuba 305-8573, Japan

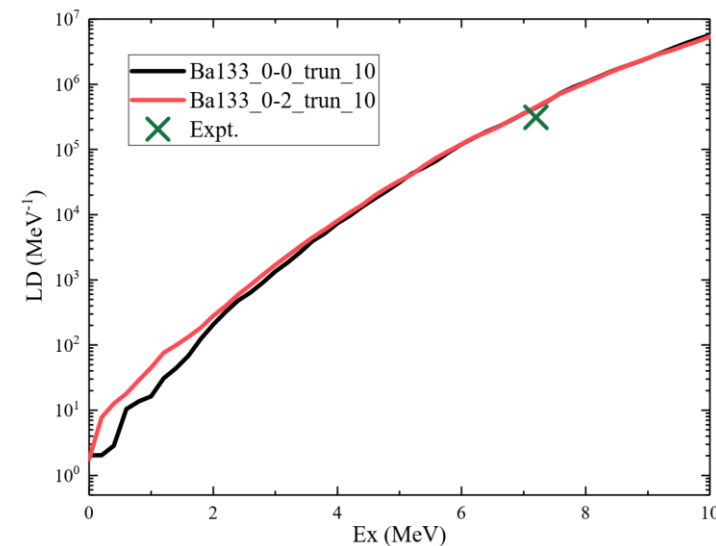
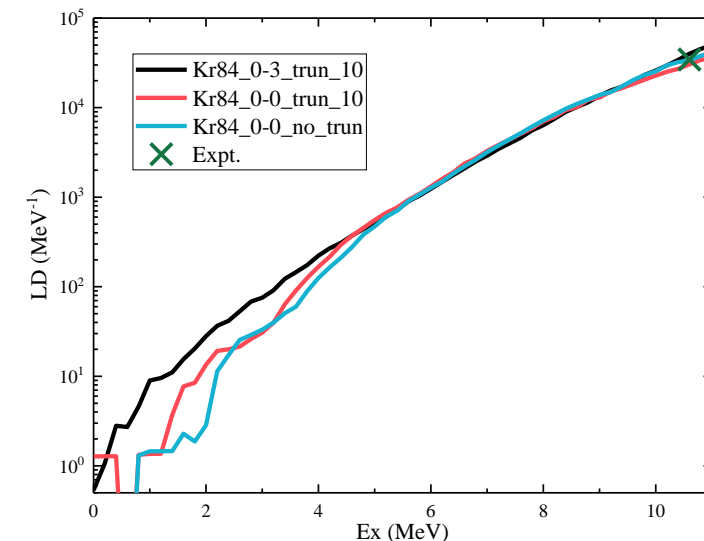
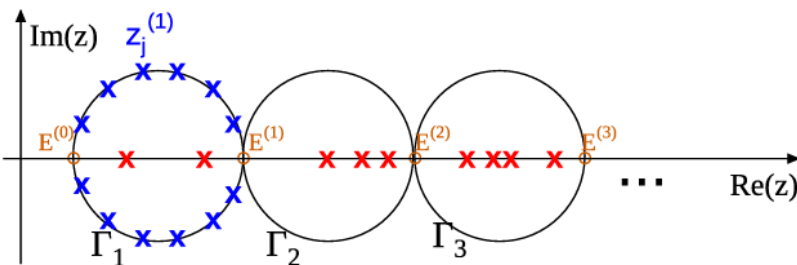
^d CREST, Japan Science and Technology Agency, Kawaguchi 332-0012, Japan

^e Institute of Natural Sciences, Senshu University, Tokyo 101-8425, Japan

^f Department of Physics, the University of Tokyo, Hongo, Tokyo 113-0033, Japan

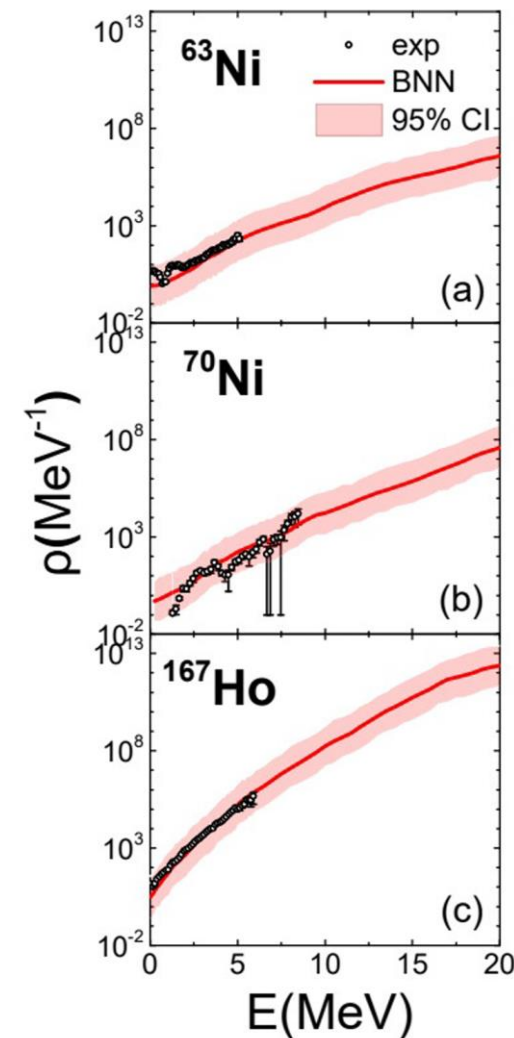
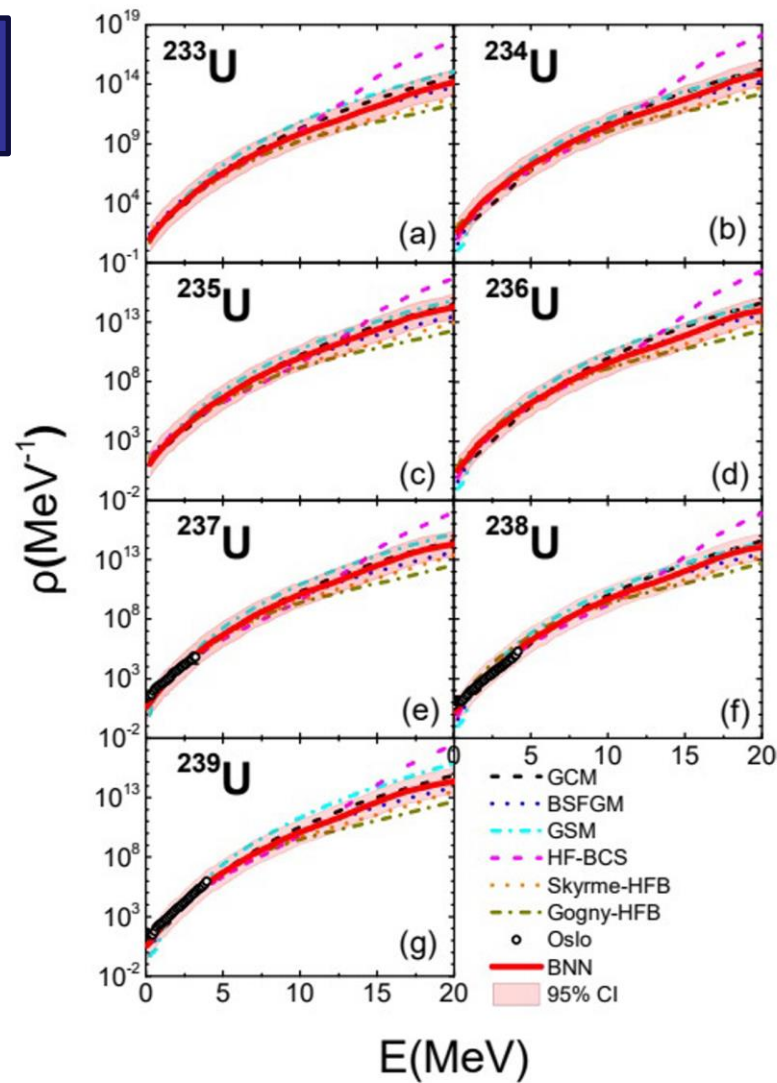
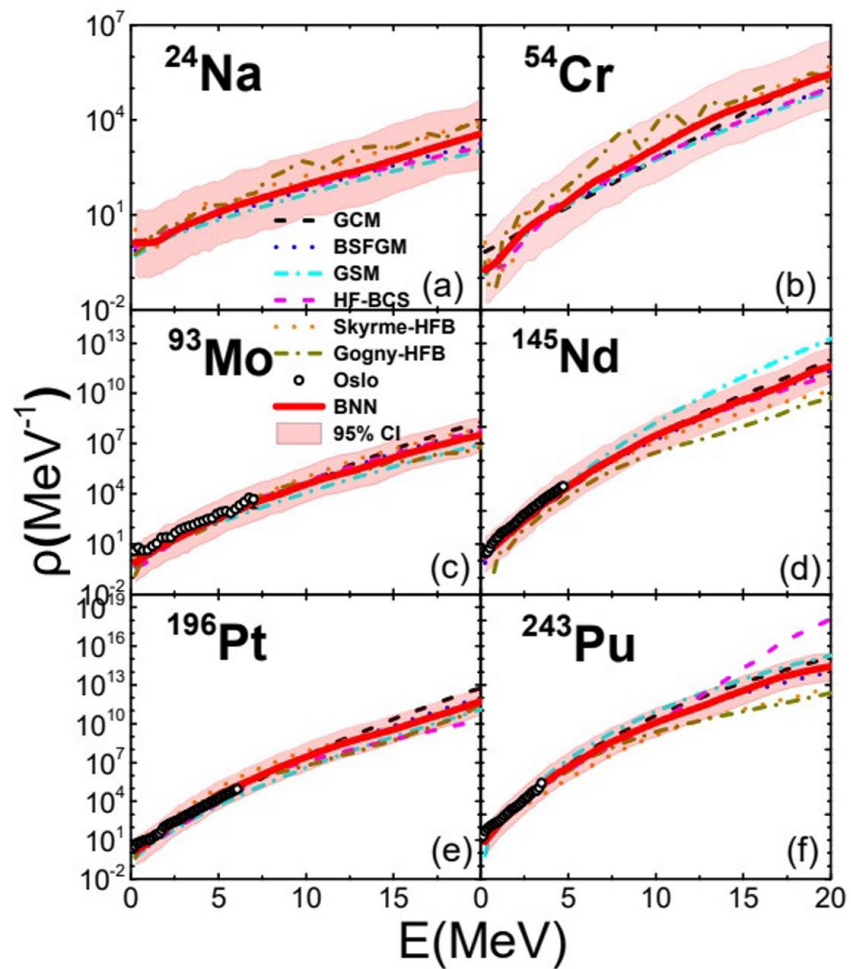
^g National Superconducting Cyclotron Laboratory, Michigan State University, East Lansing, MI 48824, USA

^h Instituut voor Kern- en Stralingsfysica, Katholieke Universiteit Leuven, B-3001 Leuven, Belgium



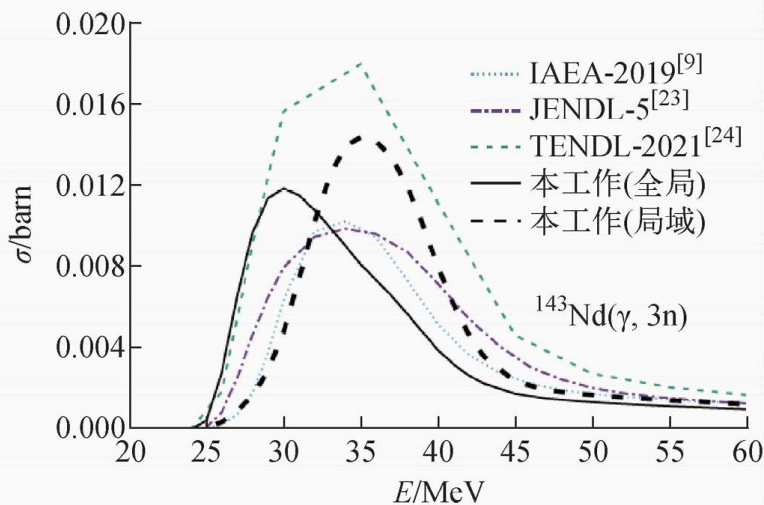
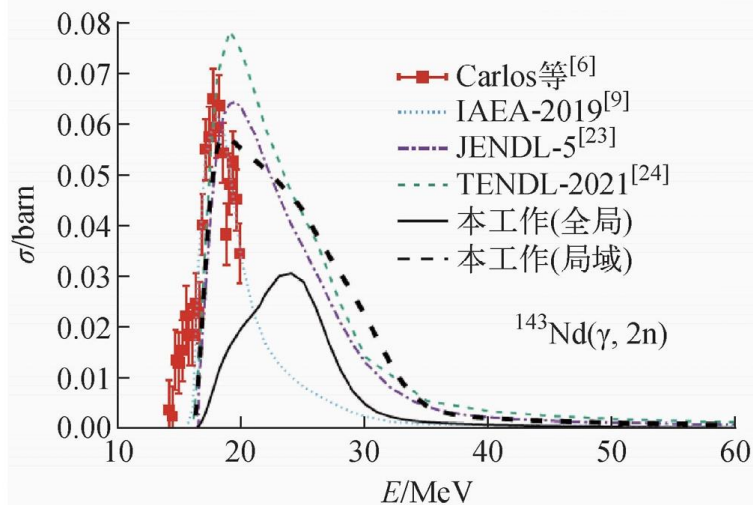
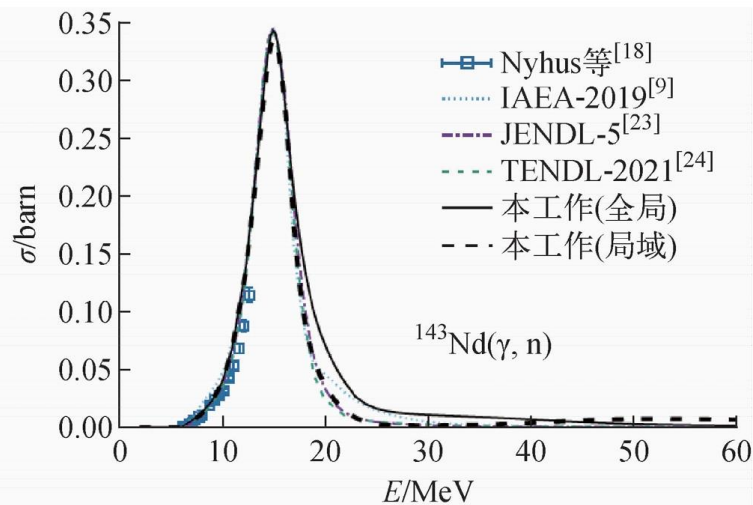
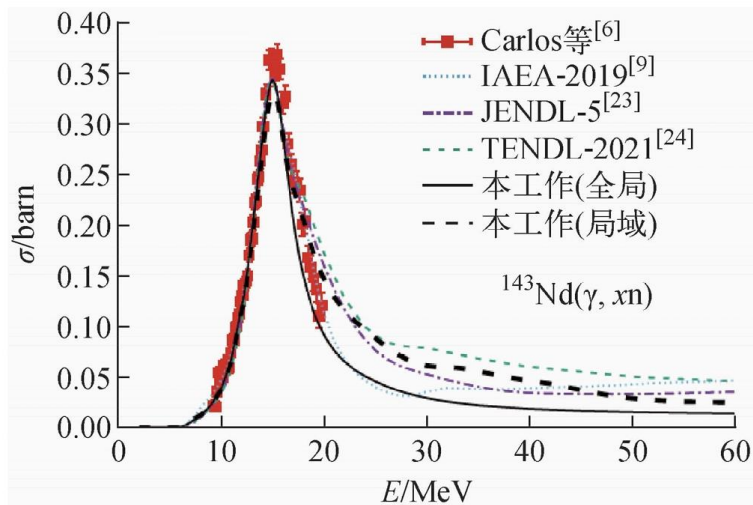
Collaborate with Prof. Yuan from ZhongShan University

Uncertainties of nuclear level density estimated using Bayesian neural networks



Chinese Physics C Vol. 48, No. 8 (2024) 084105

Application for Nd isotope



3.1 The GCCI (Gilbert-Cameron-Cook-Ignatyuk) level density parameter^[37]

$$a = a_c \frac{1 - e^{-u}}{u} + a_1 \left(1 - \frac{1 - e^{-u}}{u} \right), \quad (19)$$

where $u = f_{ued}(U - \Delta)$

$$a_c = \begin{cases} A/8.0, & \text{if } Z < 9 \text{ or } N < 9, \\ A(A_{ss} \cdot S + Q_b), & \text{for other nuclei,} \end{cases} \quad (20)$$

$$a_1 = (aif1 - aif2 \cdot A)A, \quad (21)$$

$$\text{or } a_1 = (aif1 \cdot A + aif2 \cdot A^{2/3}), \quad (22)$$

Z , N and A are the number of charge, neutron and mass of the compound nucleus, respectively; U , Δ

and S are the excited energy, pair energy and shell correction, respectively. f_{ued} , $aif1$, $aif2$ can be taken as adjustable parameters in some range, usually $f_{ued} = 0.05$; for Eq. (21), $aif1 = 0.1375$, $aif2 = 8.36 \times 10^{-5}$ ^[37]; for Eq. (22), $aif1 = 0.073$, $aif2 = 0.115$ ^[40], or $aif1 = 0.0666$, $aif2 = 0.2587$ ^[41].

$$Q_b = \begin{cases} 0.142 & \text{for spherical nuclei} \\ 0.12 & \text{for deformed nuclei} \end{cases}, \quad (23)$$

$$A_{ss} = \begin{cases} 0.00917, & \text{for Cameron-Cook}^{[38]} \\ 0.0088, & \text{for Su Zongdi}^{[39]} \end{cases}. \quad (24)$$